Polysaccharide-Stabilized Pd-Ag Nanocatalysts for Hydrogenation of 2-Hexyn-1-Ol

Alima Kainekeyevna Zharmagambetova , Eldar Talgatuly Talgatov , Assemgul Seitkhanovna Auyezkhanova * , Farida Umarovna Bukharbayeva , Aigul Iembergenovna Jumekeyeva

Posted Date: 30 August 2023

doi: 10.20944/preprints202308.2061.v1

Keywords: hydrogenation; palladium-silver catalysts; polysaccharide; 2-hexyn-1-ol

Article

Polysaccharide-Stabilized PdAg Nanocatalysts for Hydrogenation of 2-Hexyn-1-Ol

Alima K. Zharmagambetova, Eldar T. Talgatov, Assemgul S. Auyezkhanova *, Farida U. Bukharbayeva and Aigul I. Jumekeyeva

D.V. Sokolsky Institute of Fuel, Catalysis, and Electrochemistry, Laboratory of Organic Catalysis, Kunaev str. 142, 050010, Almaty, Kazakhstan; a.zharmagambetova@ifce.kz (A.K.Z); e.talgatov@ifce.kz (E.T.T.); farida.isakova1992@gmail.com (F.U.B.); jumekeeva@mail.ru (A.I.J.)

* Correspondence: auyezkhanovaa@gmail.com

Abstract: A new one-pot green technique was used for preparation of polysaccharide-based Pd- and PdAg nanocatalysts. The catalysts were obtained by sequential supporting natural polymer (2-hydroxyethyl cellulose (HEC), chitosan (Chit), pectin (Pec)) and metals on zinc oxide. The nanocatalysts based on polysaccharide were studied by various physicochemical methods (IR spectroscopy, transmission electron microscopy, X-ray powder diffraction, etc.). The catalyst characterization results indicated complete adsorption of polysaccharide and metal ions on inorganic support (ZnO). The formation of polysaccharide-stabilized Pd nanoparticles with size of ~2 nm was demonstrated. The metal nanoparticles are uniformly located on the surface of zinc oxide modified by polysaccharide. The synthesized catalysts were tested in liquid-phase hydrogenation of 2-hexyn-1-ol under mild conditions (0.1 MPa, 40 °C). Close conversion values of 2-hexyn1-ol were obtained on all developed catalysts. The selectivity to cis-hexen-1-ol of the polysaccharide-based PdAg nanocatalysts varies as follows: PdAg-HEC/ZnO > PdAg-Pec/ZnO > PdAg-Chit/ZnO. The optimum reaction temperature and catalyst loading for the PdAg catalysts modified with HEC and Chit have been determined (40 °C, 0.05 g).

Keywords: hydrogenation; palladium-silver catalysts; polysaccharide; 2-hexyn-1-ol

1. Introduction

According to requirements of green chemistry, the study of nontoxic natural polymers to create new environmentally friendly nanomaterials and stabilized metal nanoparticles for wide purposes is in the focus of researcher's interest [1–9]. Polysaccharides derived from natural sources are suitable alternatives to synthetic polymers produced from petroleum products [5–9]. Polysaccharides have different functional groups in their structure and therefore are able to form composites with mineral sorbents [10–15] and transition metal ions [15–18].

For example, the hydroxyl and amino groups in chitosan structure, interacting with transition metal ions, form metal nanoparticles, which are very promising as catalysts [19,20]. The multifunctionality of pectin (Pec) is due to the nature of its molecule consisting of linear chains of 1,4-linked residues of α-d-galacturonic acid [3,21–23] with a large number of -OH-, -COOH- groups allows its use in the design of various polymer-inorganic materials such as nanocatalysts [3], sorbents for wastewater treatment [4], thickeners, emulsifiers, gelling agents for food industry and biomedicine [21–23].

The cellulose is the most common natural polysaccharide. Its soluble derivative 2-hydroxyethyl cellulose (HEC) is formed by treating cellulose with alkali and reacting with ethylene oxide [24]. The advantages of this derivative are good water solubility, biodegradability, biocompatibility and film formation [25–28]. It is widely used in pharmaceuticals [29], textile industry [30], paper making [31], cosmetology [32], etc.

 doi:10.20944/preprints202308.2061.v1

The use of polysaccharides as new auxiliary materials for design of heterogeneous catalysts is on the rise. Chitosan (Chit) is started to use [8], mainly due to its high affinity for metal ions [20]. A number of works are devoted to catalysts for processes such as hydrogenation [1,33,34], oxidation [3,4], coupling reaction and other possible catalytic syntheses [8,19,20,35]. There are few data on pectin-containing catalysts, their design and use as stabilizer for metal nanoparticles [2–4,36–39].

Different types of cellulose were used as supports for catalysts for hydrogenation, oxidation, dye reduction, coupling reactions [3,4,35,40–43]. Bearing abundant reactive -OH groups on its chains, HEC can acts as both reducing agent for transition metal ions and stabilizing agent for metal nanoparticles formed. Despite the fact that HEC is an attractive biopolymer [44–46], its full potential for use in the design of heterogeneous catalysts has not yet been adequately developed [47–49].

To take into account the growing need of environmental friendly nanocatalyst syntheses, this work aims to prepare polysaccharide containing PdAg/ZnO catalysts. The HEC, pectin and chitosan were used as green stabilizers and water was the only medium for the syntheses of the catalysts in ambient conditions without high temperature processes of calcination and reduction. To that end, we used a new green one-pot technique for catalyst synthesis by sequential supporting polysaccharide and metals on zinc oxide. In this study, we have evaluated and compared the efficiency of the developed HEC, Chit, Pec stabilized bimetallic PdAg catalysts supported on zinc oxide with that of the monometallic Pd-HEC/ZnO nanocatalyst in the hydrogenation of 2-hexyn-1-ol.

2. Results

2.1. Characterization of catalysts

Mono- and bimetallic palladium and palladium-silver catalysts modified with polysaccharides such as chitosan (Chit), 2-hydroxyethyl cellulose (HEC) and pectin (Pec) have been prepared by adsorption method in aqueous medium under ambient conditions and constant stirring. The solution of polymer and then metal salts were sequentially added into a zinc oxide suspension. The resulting composites were washed with water and dried in air. As result the following catalysts were obtained: Pd-HEC/ZnO, PdAg-HEC/ZnO, PdAg-Chit/ZnO, PdAg-Pec/ZnO.

The palladium and silver content in the catalysts was evaluated using spectrophotometry and potentiometry methods, respectively. Analysis of supernatant solution before and after sorption process showed that 91-99% of the introduced Pd and 99-100% of Ag were adsorbed on the polymer-modified ZnO. The calculated total metal content (Pd and Ag) in the obtained polymer-modified mono- and bimetallic catalysts was 0.46-0.49 wt % that close to expected value of 0.5 wt% (Table 1).

Table 1. Results of adsorption of Pd^{2+} and Ag^{+} ions on polymer modified ZnO.

Catalysts	Concentration of metal ions in mother liquor C(Me)×10^{-6}, mol L^{-1}				Degree of adsorption, %		Pd and Ag content in catalyst, %		
	Before adsorption		After adsorption						
	Pd^{2+}	Ag^{+}	Pd^{2+}	Ag^{+}	Pd^{2+}	Ag^{+}	Pd^{2+}	Ag^{+}	Total
Pd-HEC/ZnO	1889.14	-	164.36	-	91.3	-	0.4565	-	0.46
PdAg-HEC/ZnO	1416.86	465.85	98.58	0.0020	93.0	100.0	0.3489	0.1250	0.47
PdAg-Chit/ZnO	1416.86	465.85	21.16	0.0016	98.5	100.0	0.3694	0.1250	0.49
PdAg-Pec/ZnO	1416.86	465.85	45.07	1.25	96.8	99.7	0.3631	0.1247	0.49

Table 2 shows the results of elemental analysis of the catalysts. The palladium content in Pd-HEC/ZnO, PdAg-HEC/ZnO, PdAg-Chit/ZnO and PdAg-Pec/ZnO catalysts was found to be 0.49%, 0.36%, 0.44% and 0.48%, respectively. The silver content in the bimetallic PdAg-HEC/ZnO, PdAg-Chit/ZnO and PdAg-Pec/ZnO catalysts was found to be 0.18%, 0.15%, and 0.16 %, respectively. Thus, the total metal content in all catalysts was not less than 0.5 wt%, suggesting the almost complete adsorption of metals (Pd and Ag) on the polymer modified support materials (Table 2). This is consistent with data obtained using spectrophotometry and potentiometry methods.

Preprints (www.preprints.org) | NOT PEER-REVIEWED | Posted: 30 August 2023 doi:10.20944/preprints202308.2061.v1

Table 2. Results of elemental analysis of the catalysts obtained.

Sample	Elemental composition of the catalyst, wt%		
	$Pd_{calcd/detd}$	$Ag_{calcd/detd}$	$Zn_{calcd/detd}$
Pd-HEC/ZnO	0.50/0.49	-	79.0/77.8
PdAg-HEC/ZnO	0.37/0.36	0.13/0.18	79.0/81.5
PdAg-Chit/ZnO	0.37/0.44	0.13/0.15	79.0/81.6
PdAg-Pec/ZnO	0.37/0.48	0.13/0.16	79.0/82.0

The results of X-ray powder diffraction analysis (XRD) of the ZnO, HEC/ZnO and PdAg-HEC/ZnO is shown in Figure 1. All XRD patterns showed the characteristic peaks at 37.0º, 40.2º, 42.3º,55.8º, 66.7º, 74.5º, 78.9º, 80.9º, 82.3º, 86.8º, 92.6º, which correspond to the [100], [002], [101], [102], [110], [103], [200],[112], [201], [004], [202] planes of ZnO wurtzite structure (JCPDS card no. 79-0206) [50]. A broad peak at 23º observed in polymer modified materials can be attributed to the amorphous phase of the HEC [51]. No peaks related to palladium (Pd or PdO) and silver (Ag, AgCl) species were observed on the XRD pattern of PdAg-HEC/ZnO catalyst. This can be explained by low metal (Pd, Ag) content in the catalyst and small particles sizes [52].

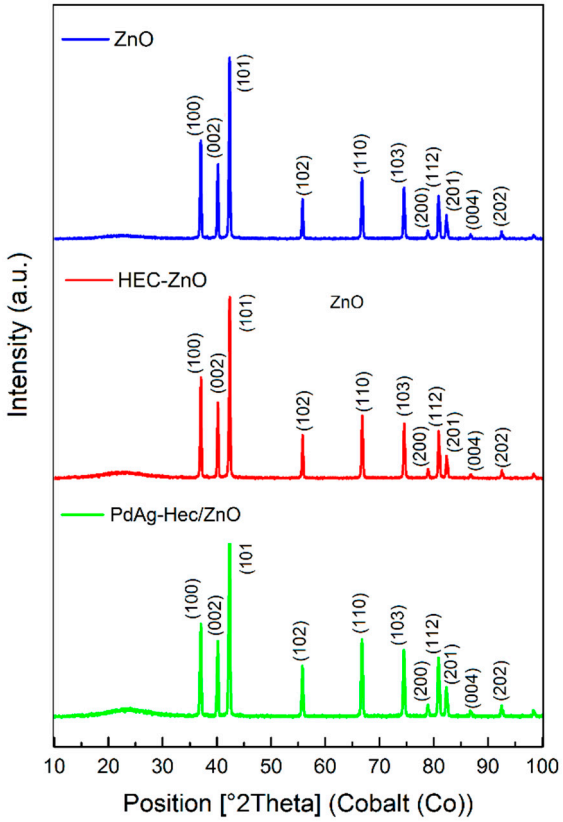

Figure 1. XRD of ZnO, HEC/ZnO and PdAg-HEC/ZnO.

The modification of ZnO with HEC is also confirmed by standardized Brunauer–Emmett–Teller (BET) method (Table 3). HEC/ZnO and PdAg-HEC/ZnO composites were characterized by decreased surface area in comparison with initial zinc oxide. It should be noted that PdAg-HEC/ZnO catalyst demonstrated the higher surface area to compare with that of HEC/ZnO composite. This is consistent with data obtained for similar systems modified with polyvinylpirollidone (PVP) [53]. In [53] decreasing the surface area from ZnO to PVP/ZnO explained by blockage of micropores in inorganic material after modification with the polymer, while increasing the surface area from PVP/ZnO to Pd-PVP/ZnO explained by a decreasing the surface coverage of the ZnO with PVP shell through changing in an orientation of the polymer functional groups from ZnO to Pd. Another explanation for such changing the surface area from unmodified zinc oxide to polymer-modified catalyst can be

Preprints (www.preprints.org) | NOT PEER-REVIEWED | Posted: 30 August 2023 doi:10.20944/preprints202308.2061.v1

in changing the degree of agglomeration of ZnO particles after modification with a polymer and following adsorption of metal ions on the polymer/ZnO composite. That is, adding of HEC solution to zinc oxide suspension can lead to agglomeration of ZnO particle probably due to ZnO-HEC-ZnO bonding. Adsorption of metal ions on HEC/ZnO composite, on the contrary, can lead to decrease the agglomeration of ZnO particles due to formation ZnO-HEC-Pd(Ag) bonds. It should be noted that according to these assumptions, HEC can interact with both zinc oxide and metal (Pd and Ag) ions.

Table 3. Surface area of ZnO, HEC/ZnO and PdAg-HEC/ZnO.

Sample	Surface area, $m^2 g^{-1}$
ZnO	8.7
HEC/ZnO	1.1
PdAg-HEC/ZnO	5.2

The interaction of the polysaccharide with other components of PdAg-HEC/ZnO catalyst and formation of polymer-metal complex on ZnO surface was confirmed by infrared spectroscopy (IRS). Figure 2 shows the IR spectra of HEC, HEC/ZnO and PdAg-HEC/ZnO. HEC shows characteristic bands at 1061 and 1122 cm^{-1}, corresponding to the C-O-C stretching vibrations in the glucopyranose structure and C-O anti-symmetric vibrations, respectively.

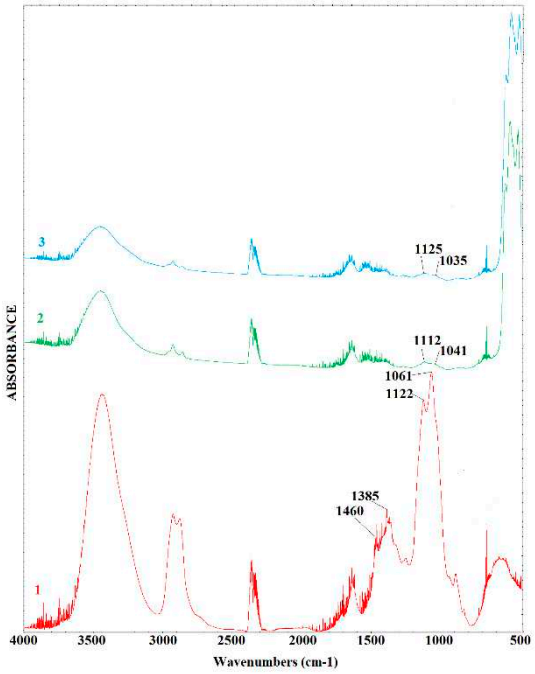

Figure 2. IR spectra of the HEC **(1)**, HEC/ZnO **(2)** and PdAg-HEC/ZnO **(3)**.

Other characteristic bands at 1460 and 1385 cm^{-1}, have been attributed to O-H "plane deformation" and for C-H "symmetric bending vibrations" respectively in -CH_2O- [54,55]. The shifting of absorption bands of O-H, C-O-C, C-O and -CH_2O- groups in the IR spectrum of the catalyst, compared to the same bands in HEC and HEC/ZnO (Figure 2, spectra 1 to 3), confirms the interaction of HEC with both ZnO and Pd (or Ag) ions.

In our prior studies [53,56] have been shown that interaction of polymers with metal ions on a support surface led to formation smaller active phase nanoparticles (~2 nm) to compare with those in similar unmodified supported catalysts. The transmission electron microscopy (TEM) image of Pd-HEC/ZnO catalyst showed the formation of finely dispersed palladium nanoparticles of ~2 nm evenly distributed on the surface of zinc oxide modified with HEC (Figure 3). This confirms the stabilization role of the polysaccharide immobilized on ZnO.

Preprints (www.preprints.org) | NOT PEER-REVIEWED | Posted: 30 August 2023 doi:10.20944/preprints202308.2061.v1

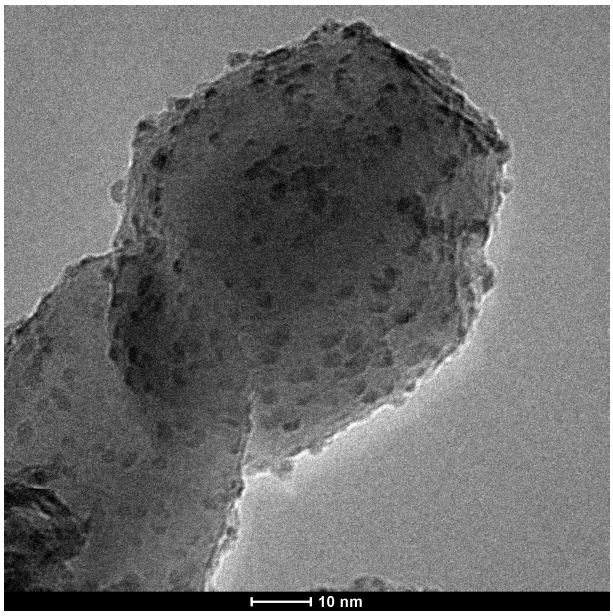

Figure 3. TEM microphotograph of Pd-HEC /ZnO catalyst.

The study of the Pd-HEC/ZnO catalyst using X-ray photoelectron spectroscopy (XPS) also confirms the presence of both polysaccharide and palladium on the surface of zinc oxide (Figure 4).

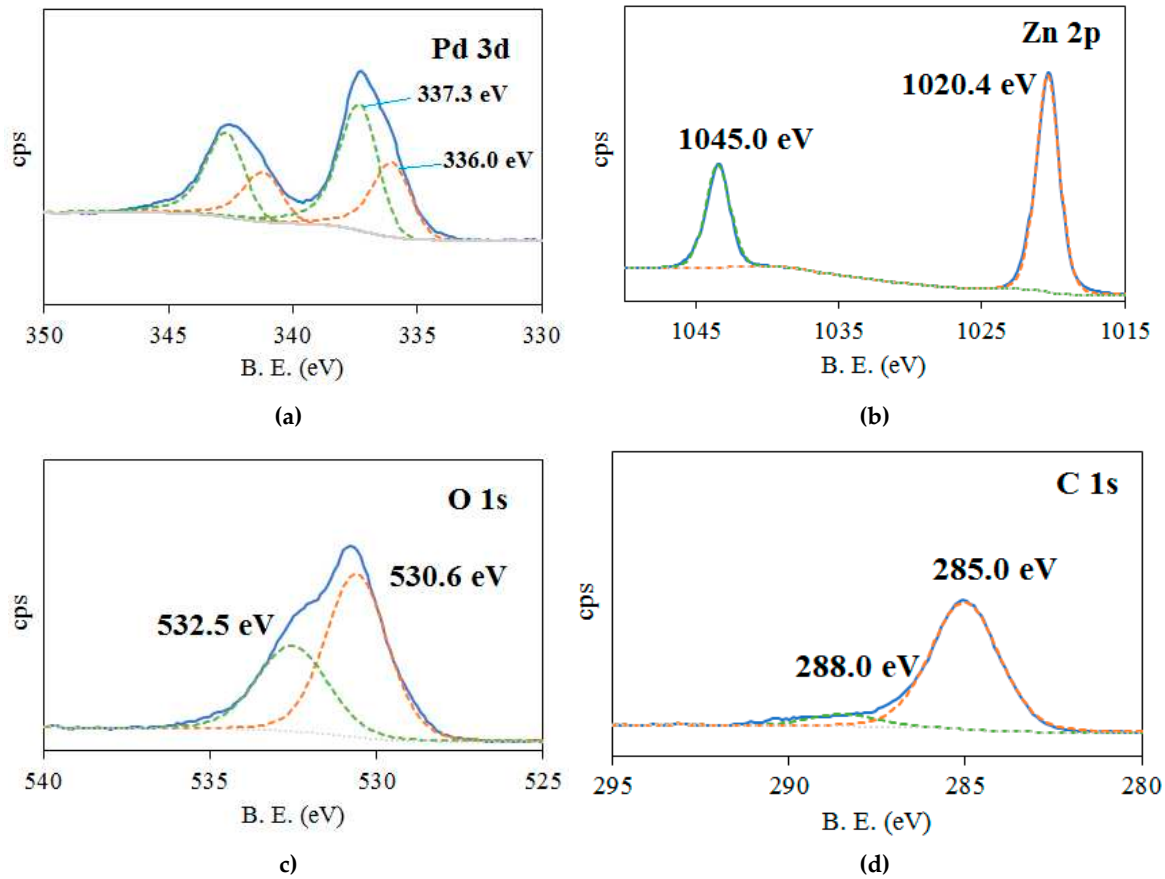

Figure 4. The lines of the Pd 3d(5/2) **(a)**, Zn 2p(3/2) **(b)**, O 1s **(c)** and C 1s **(d)** from the XPS spectrum of the Pd-HEC/ZnO catalyst.

Analysis of XPS spectrum of the Pd 3d(5/2) region (Figure 4a) showed that palladium in the catalyst occurred in both oxidized (Pd^{2+}) and reduced (Pd^{0}) states with the binding energies of ~337.3

Preprints (www.preprints.org) | NOT PEER-REVIEWED | Posted: 30 August 2023 doi:10.20944/preprints202308.2061.v1

and ~336.0 eV, respectively [57]. The presence of the small amount of zero-valent palladium is probably caused by the photocatalytic reduction of Pd^{2+} in the presence of zinc oxide, which is known as an efficient photocatalyst [58]. This suggests that a small part of the introduced palladium interacts with zinc oxide. This is confirmed by the fact that binding energy of Pd^0 has a positive shift (ca. 0.6 eV) due to strong metal-support interaction and formation of PdZn species [59]. In the case of palladium in oxidized state such shifting was not observed, confirming stabilization of PdO particles with the polymer. The peak of the Zn 2p(3/2) at 1020.4 eV corresponds to Zn^{2+} ions in a zinc oxide crystal lattice (Figure 4b) [60]. The XPS spectrum of the O 1s region (Figure 4c) was de-convoluted into two peaks with binding energies at 530.6 (peak 1) and 532.5 eV (peak 2). According to the literature data [61], peak 1 is related to O^{2-} ions in the Zn-O bonding of the wurtzite structure, and peak 2 is attributed to oxygen of OH groups on the zinc oxide surface. Peak 2 can also be assigned to the C-O oxygen in the HEC repeated unit [62]. The de-convolution of the C 1s line in the XPS spectrum of the catalyst indicated that carbon is represented by two components (Figure 4d). The main component centered at 285.0 eV is attributed to C-C bond in HEC macromolecule and no shifting of binding energy for this peak is observed. In case of the minor peak at 288.0 eV related to C-O bond in HEC some positive shift of binding energy (ca. 1.3 eV) was observed probably due to the interaction of C-O-C, C-O and -CH_2O- groups of HEC with both Pd^{2+} and Zn^{2+} of zinc oxide [62].

Thus, the characterization of polysaccharide modified catalysts using physical chemical methods such as spectrophotometry, potentiometry, elemental analysis, XRD, IRS, BET, TEM and XPS indicated that polysaccharides and metal (Pd, Ag) ions quantitatively adsorbed on zinc oxide and the polymers interacted with both ZnO and active phase particles formed. The role of polymers is both to fix Pd and Ag species on zinc oxide surface and their stabilization. This is consistent with data obtained in our prior study for similar Pd-PVP/ZnO catalyst [53]. However, in case of Pd-HEC/ZnO a small amount of Pd was also interacted with ZnO forming PdZn species. This can be explained by lesser affinity of HEC functional groups to metal ions in comparison with those of PVP.

2.2. Catalytic test

The obtained palladium and palladium-silver catalysts modified with natural polysaccharides (chitosan (Chit), 2-hydroxyethyl cellulose (HEC) or pectin (Pec)) were tested in hydrogenation process under mild conditions (0.1 MPa, 40 °C). The hydrogenation of 2-hexyn-1-ol was chosen as the model reaction. The possible pathways of the reaction are illustrated in Scheme 1. The first step triple bond of the alkynol is reduced to C=C double one forming cis/trans-isomers which then hydrogenated to alkanol.

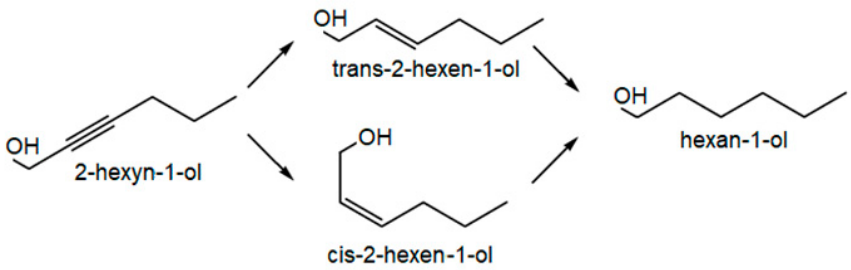

Scheme 1. Hydrogenation of 2-hexyn-1-ol.

The test results of the developed catalysts in the hydrogenation process of 2-hexyn-1-ol are given in Table 4. Polysaccharide-containing palladium-silver catalysts were found to be effective in this process. In descending order of influence on the hydrogenation rate, the stabilizing polymers form the following series: HEC > Pec > Chit (Figure 5). However, the maximum reaction rate is achieved on monometallic Pd catalysts modified with HEC (Table 4), probably due to the higher palladium content. The introduction of silver into the HEC-containing catalyst improved selectivity to 2-hexen-1-ol to compare with the selectivity on monometallic Pd catalyst (Figure 6). The cis-alkenol selectivity

Preprints (www.preprints.org) | NOT PEER-REVIEWED | Posted: 30 August 2023 doi:10.20944/preprints202308.2061.v1

of process is maximal on PdAg catalyst containing HEC and achieves 97.2%. Thus, the maximum yield of the alkenol was observed on the bimetallic PdAg catalyst stabilized with HEC and reached 89.4% at 93.0% conversion (Table 4).

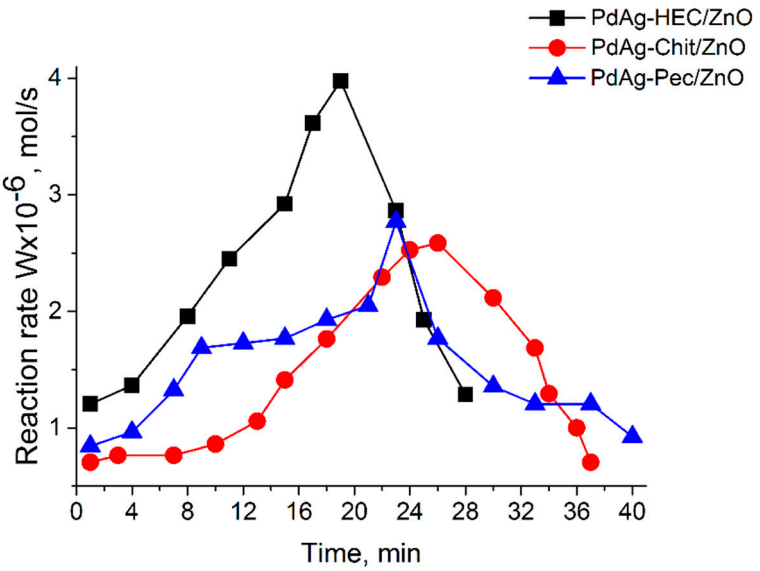

Figure 5. The rate of 2-hexyn-1-ol hydrogenation on the PdAg/ZnO catalysts modified with hydroxyethyl cellulose (HEC), chitosan (Chit) and pectin (Pec). Reaction conditions: T = 40°C, P_{H2} = 1 atm, m_{cat} = 0.05 g, ethanol = 25 mL, and $C_{alkynol}$ = 0.09 mol/L.

Table 4. The results of 2-hexyn-1-ol hydrogenation on PdAg/ZnO catalysts stabilized with hydroxyethyl cellulose (HEC), chitosan (Chit) and pectin (Pec).*

Catalysts	W_{max}·10^{-6} (mol s^{-1})	Maximum yield of cis-hexen-1-ol, %	$S_{cis\text{-}hexen\text{-}1\text{-}ol}$,%	Conversion, %
Pd-HEC/ZnO	4.3	82.8	90.6	91.4
PdAg-HEC/ZnO	4.0	89.4	97.2	93.0
PdAg-Chit/ZnO	2.6	85.9	92.3	93.1
PdAg-Pec/ZnO	2.8	86.4	93.5	92.4

*Reaction conditions presented in Figure 5.

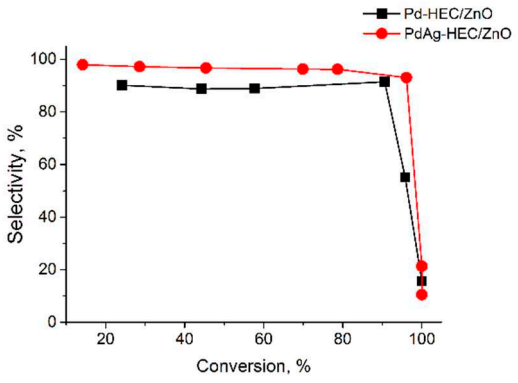

Figure 6. Selectivity of 2-hexen-1-ol vs. conversion of 2-hexyn-1-ol on Pd-HEC and PdAg-HEC catalysts supported on ZnO. Reaction conditions presented in Figure 5.

The optimum temperature and catalyst loading for the PdAg catalysts modified with HEC and Chit have been determined (Table 5). The initial reaction rate increased with increasing temperature up to 40°C.

Preprints (www.preprints.org) | NOT PEER-REVIEWED | Posted: 30 August 2023 doi:10.20944/preprints202308.2061.v1

Table 5. Effect of variation of temperature and catalyst loading on reaction conditions in hydrogenation of 2-hexyn-1-ol (0.09 mol/L) in ethanol (25 mL).

Reaction parameters	Catalysts					
	PdAg-Chit/ZnO			PdAg-HEC/ZnO		
	$W_{max}\cdot10^{-6}$ (mol s^{-1})	Maximum yield of cis-hexen-1-ol, %	$S_{cis\text{-}hexen\text{-}1\text{-}ol}$, %	$W_{max}\cdot10^{-6}$ (mol s^{-1})	Maximum yield of cis-hexen-1-ol, %	$S_{cis\text{-}hexen\text{-}1\text{-}ol}$, %
Temperature, °C						
20	0.6	84.0	91.8	0.4	77.0	93.0
30	2.3	76.4	93.5	1.3	75.6	84.9
40	**2.6**	**85.9**	**92.3**	**4.0**	**89.4**	**97.2**
50	2.3	79.3	79.8	1.6	76.2	86.7
Catalyst loading, g						
0.01	0.6	62.0	67.8	0.5	58.4	63.2
0.03	1.9	71.8	84.7	**2.5**	**88.2**	**89.8**
0.05	**2.6**	**85.9**	**92.3**	**4.0**	**89.4**	**97.2**
0.10	2.8	83.5	89.9	4.4	87.6	94.5

Further temperature increase to 50°C lead to a significant decrease in the reaction rate, which could be explained by the shrinking the surface polymer layer of the catalyst and blocking the active centers [53].

The increase in the catalyst loading from 0.01 g to 0.1 g leads to the increase in the reaction rate. The highest rate was achieved on the 0.1 g load of the both catalysts. At the same time, the maximum yield and selectivity to cis-hexene-1-ol decreased, probably due to accelerated hydrogenation of double bond of the cis-alkene into an alkane.

According to the chromatographic analysis, in the presence of HEC-modified catalyst, the conversion of 2-hexyn-1-ol to cis-2-hexen-1-ol bigan in the first half of the process (Figure 7a). After almost complete disappearance of acetylenic alcohol in the reaction medium, a process of isomerisation of cis-alkenol to trans-form is initiated and parallel reduction of double bond of alkenols to saturated alcohol is performed. A similar change in the composition of the reaction mixture is observed when the process is carried out with the catalyst containing chitosan. A little difference is that the isomerization of cis- to trans-2-hexen-1-ol on this catalyst starts slightly before the complete conversion of the initial alkynol (Figure 7b).

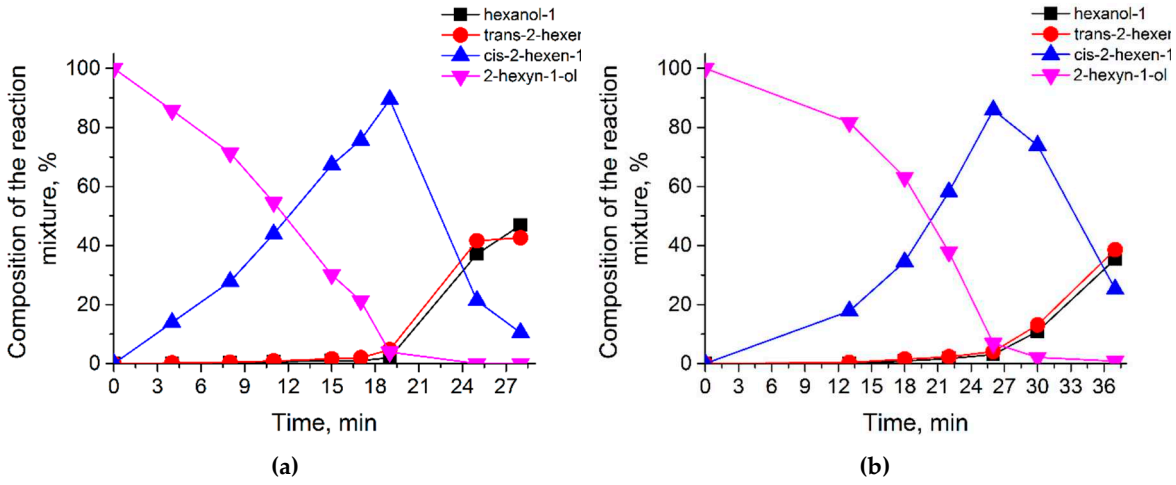

Figure 7. Changes in the composition of the reaction mixture at the hydrogenation of 2-hexyn-1-ol in the presence of PdAg-HEC/ZnO (a) and PdAg-Chit/ZnO (b). Reaction conditions presented in Figure 5.

Reusability of PdAg-Chit/ZnO and PdAg-HEC/ZnO catalysts was studied by hydrogenation of successive portions of 2-hexyn-1-ol on one the same load of catalyst (Figure 8). High stability

Preprints (www.preprints.org) | NOT PEER-REVIEWED | Posted: 30 August 2023 doi:10.20944/preprints202308.2061.v1

demonstrated by reaction rate on the both catalysts remains nearly the same at least in 10 runs demonstrating high stability. This can be explained by swelling ability of polymer-metal shell of the catalysts in ethanol and negligible leaching active phase by preventing effect of the polymers [53].

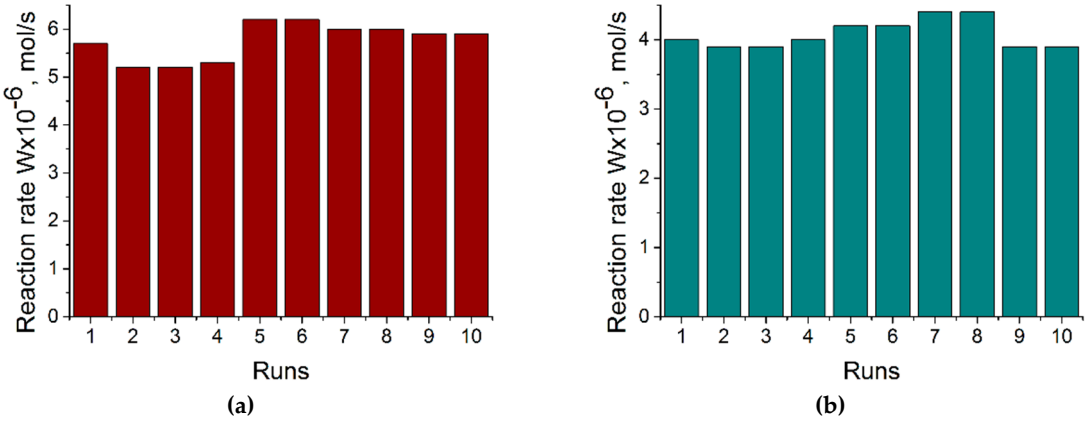

Figure 8. Hydrogenation of 10 portions of 2-hexyn-1-ol on in PdAg-Chit/ZnO **(a)** and PdAg-HEC/ZnO **(b)**. Reaction conditions presented in Figure 5.

Thus, a comparison of the performance of palladium and palladium-silver catalysts stabilised with derivatives of natutal polysaccharies (Table 5) as well as pectin confirms the prospectives of their use in synthesis of metal nanoparticles and further application in catalysis.

3. Materials and Methods

3.1. Materials

The 2-hexyn-1-ol, palladium chloride ($PdCl_2$, 59-60% Pd), silver nitrate ($AgNO_3$, 99.0%), potassium chloride (KCl, reagent grade), 2-hydroxyethyl cellulose (HEC, Mw 90,000), pectin (Pec, Mw 15,000), chitosan (Chit, Mw 250.000), zinc oxide (chemically pure) were acquired from Sigma-Aldrich, St. Louis, USA. Ethanol (reagent) was purchased from Talgar Alcohol LLP (Kazakhstan) and purified by distillation.

3.2. Preparation of K_2PdCl_4 precursor solution

A K_2PdCl_4 precursor solution was prepared by crushing 168.4 mg of palladium (II) chloride and 155.7 mg of KCl in an agate mortar according to procedure described in [53]. The obtained potassium (II) tetrachloropalladate was dissolved in 50 mL of distilled water. The process was carried out at 70°C and constant magnetic stirring for 2 hours. The concentration of palladium ions in the resulting solution was 0.019 M.

3.3. Synthesis of Pd-HEC/ZnO catalyst

The nanocatalyst was prepared by adsorption method, according to procedure described in [53,56]. A 5 mL water solution of 0.9×10^{-2} M 2-hydroxyethylcellulose (HEC, 0.0192 g in 5 mL of water) was added dropwise to the aqueous suspension of inorganic sorbent (1 g ZnO in 15 mL of water) and stirred for 2 hours. Then 5 mL of a 0.9×10^{-2} M water solution of potassium (II) tetrachloropalladate was added. The process was carried out at room temperature and constant stirring for 3 hours. The concentration of 2-hydroxyethylcellulose and potassium (II) tetrachloropalladate solutions corresponding to a palladium content of 0.5% and a molar ratio of [Pd:HEC] = 1:1. The synthesized catalyst was kept in the mother liquor for 12-15 hours. Then washing with distilled water and air drying were carried out. The amount of immobilized palladium was monitored by photoelectrocolorimetry.

 doi:10.20944/preprints202308.2061.v1

3.4. Synthesis of PdAg-polysaccharide/ZnO catalysts

The method of polysaccharide adsorption on an inorganic sorbent followed by metal ions deposition was used to prepare 0.5% bimetallic PdAg polysaccharide-inorganic nanocatalysts [53,56]. 5 mL of 0.9×10^{-2} M polysaccharide solution (HEC, Chit or Pec) was added to the aqueous suspension of the support (1 g ZnO in 15 mL of water). The preparation process was carried out at room temperature and constant stirring for 2 h. After that, aqueous solutions of palladium and silver salts (K_2PdCl_4 and $AgNO_3$) were added under constant stirring. The duration of the process was 3 h. The concentration of potassium (II) tetrachloropalladate and silver (I) nitrate water solutions corresponded to 0.5% metal content (Pd:Ag ratio = 3:1). The amount of polymer for catalyst preparation was calculated at the rate of one transition metal atom per monomer unit. After keeping the synthesized nanocatalyst in the mother liquor for 12-15 h, it was washed with distilled water and dried in air. The completeness of palladium and silver fixation was monitored by photoelectrocolorimetry and direct potentiometry, respectively.

3.5. Characterization of catalysts [53,56]

The concentration of metals (Pd, Ag) in nanocatalysts was monitored by the change in the concentration of palladium and silver ions in aqueous solution before and after immobilization of Ag+ and/or $PdCl_4^{2-}$ on an inorganic support (ZnO) modified with polysaccharide. The quantitative content of Pd in aqueous solutions was detected by photoelectrocolorimetry (PEC). The measurement was carried out on spectrophotometer SF-2000 UV/Vis (OKB "Spektr", Russia) according to the calibration curves (wavelength λ = 425 nm). Ag concentration in aqueous solutions was monitored by potentiometric method (direct potentiometry method). The measurement was carried out on an ANION 4100 ionometer ("Infraspak-Analit", Russia), using an ion-selective electrode ELIS-131Ag.

A powder X-ray diffractometer DRON-4-0.7 (Burevestnik, Russia) with monochromatized radiation of cobalt Co-Kα (λ = 0.179 nm) was used to obtain powder X-ray diffractograms.

The specific surface area and pore size distribution of the obtained nanocatalysts were investigated using the low-temperature N_2 adsorption-desorption method. The study was carried out on an Accusorb instrument (Micromeritics, USA).

The catalyst samples were studied by FTIR spectroscopic method. A Nicolet iS5 instrument (Thermo Scientific, USA) was used to study the samples by FTIR spectroscopy, in the 4000-400 cm^{-1} region. A mixture of 1 mg of sample with 100 mg of dry potassium bromide was ground to obtain pellets for IR analysis. The mixture was then pressed in a mold.

Transmission electron microscopy (TEM) micrographs were obtained on a JEM-2100 transmission electron microscope (Jeol, Japan) with an accelerating voltage of 100 kV. The elemental analysis of the nanocatalysts was performed on a JSM-6610LV scanning electron microscope with EDX detector (Jeol, Japan).

Nanocatalysts were investigated by X-ray photoelectron spectroscopy (XPS) on a Kratos Axis Ultra DLD photoelectron spectrometer (Kratos Analytical LTD, UK).

3.6. Hydrogenation of 2-hexyn-1-ol

The hydrogenation process was carried out in a thermostated glass reactor, according to procedure described in [53]. The reaction was carried out in ethanol medium (25 mL) at atmospheric hydrogen pressure, temperature of 20-50°C and intensive stirring (600-700 oscillations per minute). Before hydrogenation, the nanocatalyst (0.05 g) was reduced with hydrogen in the reactor for 30 min under intensive stirring. After hydrogen treatment, 2.23 mmol (0.09 mol/L) alkynol was added to the reactor. The amount of alkynol corresponded to an uptake of 100 mL of hydrogen. The hydrogenation rate was calculated from the hydrogen uptake per unit time. For this purpose, the volume of hydrogen uptake was measured after a certain time interval using a burette connected to the reactor.

To determine the selectivity for the main products of the hydrogenation reaction, a syringe sample of the reaction mixture were taken at proper time intervals.

The hydrogenation products were analyzed by gas-liquid chromatography on a Chromos GC1000 chromatograph (Russia) with a flame ionization detector in isothermal mode. A BP21 capillary column (FFAP) with polar phase (PEG modified with nitroterephthalate) of 50 m length and 0.32 mm inner diameter was used. The column temperature was 90°C, the injector temperature was 200°C, and helium served as the carrier gas. The amount of the investigated sample was 0.2 mL. The selectivity for alkenol was calculated as the fraction of the target product in the reaction products at a given degree of substrate conversion.

To determine the stability of the catalysts, hydrogenation of successive portions of alkynol (2.23-4.46 mmol) was carried out for the same sample of nanocatalyst (0.05 g).

4. Conclusions

The PdAg/ZnO nanocatalysts modified with pectin (Pec), 2-hydroxyethyl cellulose (HEC) and chitosan (Chit) have been prepared by green one-pot method by consequent introduction of water solutions of polysaccharide and metal salts into water suspension of ZnO under ambient conditions. Study of the resulting catalysts using spectrophotometry, potentiometry, elemental analysis, XRD, IRS, BET, TEM and XPS methods indicated that polysaccharides and metal (Pd, Ag) ions quantitatively adsorbed on zinc oxide and the polymers interacted with both ZnO and active phase particles formed. In case of Pd-HEC/ZnO the interaction of a small amount of Pd with ZnO and formation of PdZn species was also observed. This suggests that by varying the polymer nature in such type catalysts is it possible to regulate the composition of active phase particles.

The catalysts have shown excellent activity in the hydrogenation of model 2-hexyn-1-ol substrate at 40^0C and 1 atm of H_2. However, in this comparative study, Pd-HEC/ZnO proved to be slightly more effective than others.

The hydrogenation reaction takes place in a swollen bulk metal-polymer surface layer that increasing lifetime of the Pd-HEC/ZnO. Thus, this catalyst combines the advantages of both homogeneous and heterogeneous catalysts.

Excellent performance at low catalyst loadings and mild reaction conditions makes polysaccharide containing metal nanocatalysts highly attractive for further improvement and testing in both hydrogenation of different types of unsaturated organic compounds and other important catalytic processes.

Author Contributions: Conceptualization, A.S.A. and A.K.Z; methodology, E.T.T.; software, F.U.B. and A.I.J.; validation and formal analysis, A.K.Z., E.T.T., A.S.A.; investigation, A.I.J. and F.U.B.; resources, A.K.Z, E.T.T. and A.S.A.; data curation, F.U.B.; writing—original draft preparation, A.K.Z, E.T.T. and A.S.A.; writing—review and editing, A.K.Z. and A.S.A.; visualization, A.I.J. and F.U.B.; supervision, project administration and funding acquisition A.K.Z. All authors have read and agreed to the published version of the manuscript.

Funding: This research was funded by the Committee of Science of the Ministry of Science and Higher Education of the Republic of Kazakhstan (Grant No. AP09259638).

Data Availability Statement: The data that support the findings of this study are available from the corresponding author upon reasonable request.

Acknowledgments: This work was carried out with the financial support of the Committee of Science of the Ministry of Science and Higher Education of the Republic of Kazakhstan (Grants No. AP09259638).

Conflicts of Interest: The authors declare no conflict of interest.

References

1. Zheng, X., Li, Y., Li, W., Pei, X., Ye, D. Chitosan derived efficient and stable Pd nano-catalyst for high efficiency hydrogenation. *International Journal of Biological Macromolecules* **2023**, *241*, 124615. doi:10.1016/j.ijbiomac.2023.124615
2. Baran, T. Pd(0) nanocatalyst stabilized on a novel agar/pectin composite and its catalytic activity in the synthesis of biphenyl compounds by Suzuki-Miyaura cross coupling reaction and reduction of o-nitroaniline. *Carbohydrate Polymers* **2018**, *195*, 45–52. doi:10.1016/j.carbpol.2018.04.064
3. Nasrollahzadeh, M., Shafiei, N., Nezafat, Z., Bidgoli, N.S.S., Soleimani, F. Recent progresses in the application of cellulose, starch, alginate, gum, pectin, chitin and chitosan based (nano)catalysts in

sustainable and selective oxidation reactions: A review. *Carbohydrate Polymers* **2020**, *241*, 116353. doi:10.1016/j.carbpol.2020.116353

4. Nasrollahzadeh, M., Sajjadi, M., Iravani, S., Varma, R.S. Starch, cellulose, pectin, gum, alginate, chitin and chitosan derived (nano)materials for sustainable water treatment: A review. *Carbohydrate Polymers* **2021**, *251*, 116986. doi:10.1016/j.carbpol.2020.116986
5. Zhu, Y., Li, Z., Chen, J. Applications of Lignin-Derived Catalysts for Green Synthesis. *Green Energy & Environment* **2019**, *4*, 210–244. doi:10.1016/j.gee.2019.01.003
6. Mahlambi, P.N., Moloto, M.J. Starch-capped silver oxide (Ag_2O) nanoparticles: synthesis, characterization and antibacterial activity. *Digest Journal of Nanomaterials and Biostructures* **2022**, *17*, 921–930. doi:10.15251/DJNB.2022.173.921
7. De Almeida, D.A., Sabino, R.M., Souza, P.R., Bonafé, E.G., Venter, S.A.S., Popat, K.C., Martins, A.F., Monteiro, J.P. Pectin-capped gold nanoparticles synthesis in-situ for producing durable, cytocompatible, and superabsorbent hydrogel composites with chitosan. *International Journal of Biological Macromolecules* **2020**, *147*, 138–149. doi:10.1016/j.ijbiomac.2020.01.058
8. Molnár, Á. The use of chitosan-based metal catalysts in organic transformations. *Coordination Chemistry Reviews* **2019**, *388*, 126–171. doi:10.1016/j.ccr.2019.02.018
9. Khazaei, A., Khazaei, M., Rahmati, S. A green method for the synthesis of gelatin/pectin stabilized palladium nanoparticles as efficient heterogeneous catalyst for solvent-free Mizoroki-Heck reaction. *J. Mol. Catal. A.* **2015**, *398*, 241–247. doi:10.1016/j.molcata.2014.12.013
10. Jafarzadeh-Moghaddam, M., Shaddel, R., Peighambardoust, S., Singh, V., Srivastava, P., Singh, A., Singh, D., Malviya, T. Polysaccharide-Silica Hybrids: Design and Applications. *Polymer Reviews* **2016**, *56*, 113–136. doi:10.1080/15583724.2015.1090449
11. Horvat, G., Pantić, M., Knez, Ž., Novak, Z. Preparation and characterization of polysaccharide-silica hybrid aerogels. *Scientific Reports* **2019**, *9*, 16492. doi:10.1038/s41598-019-52974-0
12. Abd El-Aziz, M.E., Kamal, K.H., Ali, K.A., Abdel-Aziz, M.S., Kamel, S. Biodegradable grafting cellulose/clay composites for metal ions removal. *International Journal of Biological Macromolecules* **2018**, *118*, 2256–2264 doi:10.1016/j.ijbiomac.2018.07.105
13. Abubakar, Z., Sirajo, V. Pectin graft copolymer-montmorillonite composite: Synthesis, swelling and divalent metal ion adsorption. *Separation Science and Technology* **2018**, *35*, 2170–2185. doi:10.1080/01496395.2018.1446987
14. Nesi, A., Meseldzija, S., Cabrera-Barjas, G., Onjia, A. Novel Biocomposite Films Based on High Methoxyl Pectin Reinforced with Zeolite Y for Food Packaging Applications. *Foods* **2022**, *11*, 360. doi:10.3390/foods1103036010
15. Talgatov, E.T., Auezkhanova, A.S., Kapysheva, U.N., Bakhtiyrova, S.K., Zharmagambetova, A.K. Synthesis and Detoxifying Properties of Pectin-Montmorillonite Composite. *J. Inorg. Organomet. Polym.* **2016**, *26*, 1387–1391. doi:10.1007/s10904-016-0422-7
16. Wang, R., Liang, R., Dai, T.T., Chen, J. Shuai, X., Liu, C. Pectin-based adsorbents for heavy metal ions: A review. *Trends in Food Science & Technology* **2019**, *91*, 319–329. doi:10.1016/j.tifs.2019.07.033
17. Bok-Badura, J., Jakóbik-Kolon, A., Karoń, K., Mitko, K. Sorption studies of heavy metal ions on pectin-nano-titanium dioxide composite adsorbent. *Separation Science and Technology* **2018**, *53*, 1034–1044. doi:10.1080/01496395.2017.1329840
18. Li, J., Yang, Z.L., Ding, T., Song, Y.J., Li, H.C., Li, D.Q., Chen, S., Xu, F. The role of surface functional groups of pectin and pectin-based materials on the adsorption of heavy metal ions and dyes. *Carbohydr Polym*. **2022**, *276*, 118789. doi: 10.1016/j.carbpol.2021.118789
19. Kumar, S., Singhal, N., Singh, R.K., Gupta, P., Singh, R., Jain, S.L. Dual catalysis with magnetic chitosan: Direct synthesis of cyclic carbonates from olefins with carbon dioxide using isobutyraldehyde as the sacrificial reductant. *Dalton Trans.* **2015**, *44*, 11860–11866. doi:10.1039/C5DT01012H
20. Baig, R.B.N., Varma, R.S. Copper on chitosan: A recyclable heterogeneous catalyst for azide-alkyne cycloaddition reactions in water. *Green Chem*. **201**3, *15*, 839–1843. doi:10.1039/C3GC40401C
21. Singhal, S., Rachayya, N., Hulle, S. Citrus pectins: Structural properties, extraction methods, modifications and applications in food systems – A review. *Applied Food Research*. **2022,** *2*, 100215. doi:10.1016/j.afres.2022.100215
22. Bonnin, E., Garnier, C., Ralet, M.-C. Pectin-modifying enzymes and pectin-derived materials: Applications and impacts. *Applied Microbiology and Biotechnology* **2014**, *98*, 519–532. doi:10.1007/s00253-013-5388-6
23. Roman-Benn, A., Contador, C.A., Li, M.-W., Lam, H.-M., Ah-Hen, K., Ulloa, P.E., Ravanal, M.C. Pectin: An overview of sources, extraction and applications in food products, biomedical, pharmaceutical and environmental issues. *Food Chemistry Advances* **2023**, *2*, 100192. https://doi.org/10.1016/j.focha.2023.100192
24. Dong, Y., Bi, J., Zhang, S., Zhu, D., Meng, D., Ming, S., , Qin, K., Liu, Q., Guo, L., Li, T. Palladium supported on N-Heterocyclic carbene functionalized hydroxyethyl cellulose as a novel and efficient catalyst for the

Suzuki reaction in aqueous media. *Applied Surface Science* **2020,** *531,* 147392. doi:10.1016/j.apsusc.2020.147392

25. Karger-Kocsis, J., Siengchin, S. Single-polymer composites: Concepts, realization and Outlook. *KMUTNB International Journal of Applied Science and Technology* **2014**, *7*, 1–9. doi:10.14416/j.ijast.2014.01.002
26. Ahmed, H.B., Attia, M.A., El-Dars, F.M.S.E., Emam, H.E. Hydroxyethyl cellulose for spontaneous synthesis of antipathogenic nanostructures: (Ag & Au) nanoparticles versus Ag-Au nano-alloy. *International Journal of Biological Macromolecules* **2019**, *128*, 214–229. doi:10.1016/j.ijbiomac.2019.01.093
27. Liu, X., Zeng, W., Zhao, J., Qiu, X., Xiong, H., Liang, Y., Xie, Y., Ziqiang, L., Chen, D. Preparation and anti-leakage properties of hydroxyethyl cellulose-g-poly (butyl acrylate-co-vinyl acetate) emulsion. *Carbohydrate Polymers* **2021,** *255,* 117467. doi:10.1016/j.carbpol.2020.11746
28. Diao, Y., Song, M., Zhang, Y., Shi, L.Y., Lv, Y., Ran, R. Enzymic degradation of hydroxyethyl cellulose and analysis of the substitution pattern along the polysaccharide chain. *Carbohydrate Polymers* **2017**, *169*, 92–100. doi:10.1016/j.carbpol.2017.02.089
29. Abbas, K., Amin, M., Hussain, M.A., Sher, M., Bukhari, S.N.A., Jantan, I., Edgar, K.J. Designing novel bioconjugates of hydroxyethyl cellulose and salicylates for potential pharmaceutical and pharmacological applications. *International Journal of Biometeorology* **2017**, *103*, 441–450. doi:10.1016/j.ijbiomac.2017.05.061
30. Alam, M.N., Christopher, L.P. A novel, cost-effective and eco-friendly method for preparation of textile fibers from cellulosic pulps. *Carbohydrate Polymers* **2017**, *173*, 253–258. doi:10.1016/j.carbpol.2017.06.005
31. Boufi, S., Gonzalez, I., Delgado-Aguilar, M., Tarres, Q., Pelach, M.A., Mutje, P. Nanofibrillated cellulose as an additive in papermaking process: A review. *Carbohydrate Polymers* **2016**,*154*, 151–166. doi:10.1016/j.carbpol.2016.07.117
32. Ullah, H., Santos, H.A. Khan, T. Applications of bacterial cellulose in food, cosmetics and drug delivery. *Cellulose* **2016**, *23*, 2291–2314. doi:10.1007/s10570-016-0986-y
33. Tang, S., Li, L., Cao, X., Yang, Q. Ni-chitosan/carbon nanotube: An efficient biopolymer-inorganic catalyst for selective hydrogenation of acetylene. *Heliyon* **2023**, *9*, e13523. doi:10.1016/j.heliyon.2023.e13523
34. Zharmagambetova, A.K., Auyezkhanova, A.S., Talgatov, E.T., Jumekeyeva, A.I. Chitosan-Modified Palladium Catalysts in Hydrogenation of n-Hex-2-yne. *Theoretical and Experimental Chemistry* **2021**, *57*, 371–376. doi:10.1007/s11237-021-09707-0
35. Dohendou, M., Pakzad, K., Nezafat, Z., Nasrollahzadeh, M., Dekamin, M.G. Progresses in chitin, chitosan, starch, cellulose, pectin, alginate, gelatin and gum based (nano)catalysts for the Heck coupling reactions: A review. *International Journal of Biological Macromolecules* **2021**, *192*, 771–819. doi:10.1016/j.ijbiomac.2021.09.162
36. Dolinska, J., Holdynski, M., Pieta, P., Lisowski, W., Ratajczyk, T., Palys, B., Jablonska, A., Opallo, M. Noble Metal Nanoparticles in Pectin Matrix. Preparation, Film Formation, Property Analysis, and Application in Electrocatalysis. *ACS Omega* **2020**, *5*, 23909–23918. doi:10.1021/acsomega.0c03167
37. Le, V.-D., T. Le, C.-H., Chau, V.-T., Le, T.N.-D., Dang, C.-H., Vo, T.T.-N., Nguyen, T.D., Nguyen, T.-D. Palladium nanoparticles in situ synthesized on Cyclea barbata pectin as a heterogeneous catalyst for Heck coupling in water, the reduction of nitrophenols and alkynes. *New Journal of Chemistry* **2021**, *45*, 4746–4755. doi:10.1039/d0nj05032f
38. Carrera S.A., Villarreal, J.S., Acosta P.I., Noboa J.F., Gallo-Cordova, A., Mora, J.R. Designing an efficient and recoverable magnetic nanocatalyst based on Ca, Fe and pectin for biodiesel production. *Fuel* **2022**, *310*, Part C. doi:10.1016/j.fuel.2021.122456
39. Zharmagambetova, A.K., Seitkalieva, K.S., Talgatov, E.T., Auezkhanova, A.S., Dzhardimalieva, G.I., Pomogailo, A.D. Polymer-modified supported palladium catalysts for the hydrogenation of acetylene compounds. *Kinetics and Catalysis* **2016**, *57*, 360–367. doi: 10.7868/S0453881116030175
40. Li, S., He, G., Huang, J. Self-assembly on natural cellulose: Towards high-efficient catalysts. *Current Opinion in Colloid & Interface Science* **2023**, *63*, 101655. doi:10.1016/j.cocis.2022.101655
41. El Idrissi, N., Belachemi, L., Merle, N., Zinck, P., Kaddami, H. Comprehensive preparation and catalytic activities of Co/TEMPO-cellulose nanocomposites: A promising green catalyst. *Carbohydrate Polymers* **2022**, *295*, 119765. doi:10.1016/j.carbpol.2022.119765
42. Prekob, Á., Hajdu, V., Muránszky, G., Fiser B., Sycheva A., Ferenczi, T., Viskolcz, B., Vanyorek, L. Application of carbonized cellulose-based catalyst in nitrobenzene hydrogenation. *Materials Today Chemistry* **2020**, *17*, 100337. doi:10.1016/j.mtchem.2020.100337
43. Kaushik, M., Li, A.Y., Hudson, R., Masnadi, M., Li, Ch.-J., Moores, A. Reversing aggregation: direct synthesis of nanocatalysts from bulk metal. Cellulose nanocrystals as active support to access efficient hydrogenation silver nanocatalysts. *Green Chem*.-20158. doi:10.1039/C5GC01281C
44. Ahmed, H.B., Attia, M.A., El-Dars, F.M.S.E., Emam, H.E. Hydroxyethyl cellulose for spontaneous synthesis of antipathogenic nanostructures: (Ag & Au) nanoparticles versus Ag-Au nano-alloy. *International Journal of Biological Macromolecules* **2019**, *128*, 214–229. doi:10.1016/j.ijbiomac.2019.01.093

45. Liu, X., Zeng, W., Zhao, J., Qiu, X., Xiong, H., Liang, Y., Xie Y., Ziqiang, L., Chen, D. Preparation and anti-leakage properties of hydroxyethyl cellulose-g-poly (butyl acrylate-co-vinyl acetate) emulsion. *Carbohydrate Polymers* **2021**, *255*, 117467. doi:10.1016/j.carbpol.2020.11746
46. Diao, Y., Song, M., Zhang, Y., Shi, L.Y., Lv, Y., Ran, R. Enzymic degradation of hydroxyethyl cellulose and analysis of the substitution pattern along the polysaccharide chain. *Carbohydrate Polymers* **2017**,169, 92–100. doi: 10.1016/j.carbpol.2017.02.089
47. Dong, Y., Bi J., Zhang, S., Zhu, D., Meng, D., Ming, S., Qin, K., Liu, Q., Guo, L., Li, T. Palladium supported on N-Heterocyclic carbene functionalized hydroxyethyl cellulose as a novel and efficient catalyst for the Suzuki reaction in aqueous media. *Applied Surface Science* **2020**, *531*, 147392. doi:10.1016/j.apsusc.2020.147392
48. Xie, C., Qu L., Yu, H., Yu, F., Yuan B., Yu, S., Nie, S. Synthesis of Ru nanoparticles with hydroxyethyl cellulose as stabilizer for high-efficiency reduction of α-pinene. *Cellulose* **2019**, *26*, 8059–8071. doi:10.1007/s10570-019-02656-x
49. Zharmagambetova, A.K., Usmanova, M.M., Auyezkhanova, A.S., Akhmetova, S.N., Talgatov, E.T., Tumabayev, N.Zh, Dyusenalin B.K. Synthesis and catalytic properties of composites with Pd-(2-Hydroxyethylcellulose) on bentonite. *News of the national academy of sciences of the Republic of Kazakhstan. Series Chemistry and Technology* **2019**, 5, 22–29. doi:10.32014/2019.2518-1491.49
50. Devi, P.G., Velu, A.S. Synthesis, structural and optical properties of pure ZnO and Co doped ZnO nanoparticles prepared by the co-precipitation method. *J. Theor. Appl. Phys.* **2016**, *10*, 233–240. doi:10.1007/s40094-016-0221-0
51. Mukerabigwi, J. F., Lei, S., Fan, L., Wang, H., Luo, S., Ma, X., Qin J., Huan X., Cao, Y. Eco-friendly nano-hybrid superabsorbent composite from hydroxyethyl cellulose and diatomite. *RSC Advances* **2016**, *6*, 31607–31618. doi:10.1039/c6ra01759b
52. Reddy, G. K., Peck, T. C., Roberts, C. A. "PdO vs. PtO"- The Influence of PGM Oxide Promotion of Co3O4 Spinel on Direct NO Decomposition Activity. *Catalysts* **2019**, *9(1)*, 62. doi:10.3390/catal9010062
53. Talgatov, E.T., Auyezkhanova, A.S., Zharmagambetova, A.K., Tastanova, L.K., Bukharbayeva F.U., Jumekeyeva, A.I., Aubakirov, T.A. The Effect of Polymer Matrix on the Catalytic Properties of Supported Palladium Catalysts in the Hydrogenation of Alkynols. *Catalysts* **2023**, *13*, 741. doi:10.3390/catal13040741
54. Bajaber M. A., Anjum M. N., Ibrahim M., Farooq T., Ahmad M. N., Abideen Z. Synthesis and Characterization of Hydroxyethyl Cellulose Grafted with Copolymer of Polyaniline and Polypyrrole Biocomposite for Adsorption of Dyes. *Molecules* **2022**, *27(23)*, 8238. doi:10.3390/molecules27238238
55. El Idrissi, A., El Barkany, S., Amhamdi, H., Maaroufi, A.-K. Physicochemical characterization of celluloses extracted from Esparto "Stipa tenacissima" of Eastern Morocco. *J. Appl. Polym. Sci.* **2013**, *128*, 537–548. doi:10.1002/app.37500
56. Zharmagambetova, A., Auyezkhanova, A., Talgatov, E., Jumekeyeva, A., Buharbayeva, F., Akhmetova, S., Myltykbayeva, Zh., Lopez Nieto, J. M. Synthesis of polymer protected Pd–Ag/ZnO catalysts for phenylacetylene hydrogenation. *Journal of Nanoparticle Research* **2022**, *24(12)*, 1–17. doi:10.1007/s11051-022-05621-1
57. Parambhath, V.B., Nagarm, R., Ramaprabhum, S. Effect of Nitrogen Doping on Hydrogen Storage Capacity of Palladium Decorated Graphene. *Langmuir* **2012**, *28*, 7826–7833. doi:10.1021/la301232r
58. Rusinque, B., Escobedo, S., de Lasa, H. Photoreduction of a Pd-Doped Meso-porous TiO_2 Photocatalyst for Hydrogen Production under Visible Light. *Catalysts* **2020**, *10*, 74. doi:10.3390/catal10010074
59. Chen, X., Shi, C., Wang, X.B., Li, W-Y., Liangm, C. Intermetallic PdZn nanoparticles catalyze the continuous-flow hydrogenation of alkynols to cis-enols. *Commun. Chem.* **2021**, *4*, 175. doi: 10.1038/s42004-021-00612-0
60. Mintcheva, N., Aljulaih, A.A., Wunderlich, W., Kulinich, S.A., Iwamori, S. Laser-Ablated ZnO Nanoparticles and Their Photocatalytic Activity toward Organic Pollutants. *Materials* **2018**, *11*, 1127. doi: 10.3390/ma11071127.
61. Claros, M., Setka, M., Jimenez, Y.P., Vallejos, S. AACVD Synthesis and Characterization of Iron and Copper Oxides Modified ZnO Structured Films. *Nanomaterials* **2020**, *10*, 471. doi:10.3390/nano10030471
62. Johansson, L.-S., Campbell, J.M., Rojas, O.J. Cellulose as the *in situ* reference for organic XPS. Why? Because it works. *Surface and Interface Analysis* **2020**, *52*, 1134–1138. doi: 10.1002/sia.6759